Analysis of Absorption Process in a Smooth-Tube Heat Exchanger with a Porous Medium

YONG TAE KANG, RICHARD N. CHRISTENSEN, and KAMBIZ VAFAI

Department of Mechanical Engineering, The Ohio State University, Columbus, Ohio, USA

In this article the absorption process in a smooth-tube heat exchanger (GAX absorber) with a porous medium is analyzed and a countercurrent model for GAX absorber that includes an absorption process within the porous medium is proposed. The absorption process is separated into three regions, a vapor region without a porous medium (region I), a vapor region within a porous medium (region II), and a liquid region within a porous medium (region III). The effects of thermal conductivities and porosities of the porous medium on the absorption rate and the required tube length are investigated, and the Nusselt number within each region is also predicted. The results show that the absorption rate increases with an increase of the thermal conductivity and with a decrease in porosity of the porous medium. The optimum value of the ratio of thermal conductivities (k_p / k_l) was found to be 5.0, and the optimum value of the porosity was found to be larger than 0.2.

Absorption is a process that involves heat and mass transfer of a condensable vapor from the vapor phase to a liquid phase. The generator-absorber heat exchanger (GAX) cycle is an ammonia–water absorption cycle that has been worked on for many years. The GAX cycle using ammonia–water as the solution pair consists of the following components: generator, rectifier, condenser, evaporator, and absorber. The most critical component within the GAX cycle is the absorber section. The GAX absorber is assumed to have two different heat transfer modes. One is forced convection of the liquid film on the wall, and the other is absorption at the interface between the vapor and liquid. Ammonia molecules are first moved into the interface between the liquid and vapor from the bulk vapor region, across the interface, and finally into the liquid phase.

Address correspondence to Kambiz Vafai, Department of Mechanical Engineering, Ohio State University, 206 West 18th Avenue, Columbus, OH 43210-1107.

In the case of vertical countercurrent flow between the liquid and vapor, flooding phenomenon will occur when the vapor velocity is very high compared with the liquid velocity. Hewitt [1] mentioned that as the vapor velocity is gradually increased, a point is reached where large waves and disturbances occur at the wall surface, with the liquid being held up periodically by the inflow of the vapor. This flooding phenomenon may result in a large resistance to heat transfer. The pressure drop increases quite sharply near the flooding stage and continues to increase as the vapor velocity increases until the liquid flow reverses direction and moves upward.

The use of a porous medium has a profound effect in eliminating the flooding phenomenon and increasing the heat transfer coefficient in the

absorber section. For this, simultaneous fluid flow and heat transfer in porous media should be taken into account during the absorption process. Convective heat transfer in fluid-saturated porous media has gained considerable attention in recent years because of various applications involving the use of porous media such as packed-bed heat exchangers, heat pipes, thermal insulation, petroleum reservoirs, nuclear waste repositories, and geothermal engineering [2].

A number of investigations have been done on phase change in porous media. Vafai and coworkers have thoroughly studied the phase change in porous insulation. Vafai and Whitaker [3] considered the phase-change process and its effects on the temperature, vapor density, moisture content, liquid content, and the vapor pressure distributions in porous insulation. Vafai and Sarkar [4] presented an investigation of condensation effects in a fibrous insulation slab. They proposed that heat transfer augmentation due to condensation can be minimized by designing an insulation slab that has a low Lewis number. Vafai and Sozen [5, 6] and Sozen and Vafai [7] analyzed the nonthermal equilibrium condensing flow of a gas through a packed bed. Vafai and Tien [8] performed a numerical study of heat and mass transfer with phase change in porous materials. Kaviany [9] examined evaporation and condensation in porous media and Cheng [10] investigated film condensation along an inclined surface in a porous medium, and proposed a similarity solution for the condensation problem.

However, while Vafai and co-workers considered the condensation in forced-convective flow within a porous slab as well as the condensation and evaporation process in natural convection within cavities, no literature has been found for the phase change of binary mixtures within porous media. In the case of binary mixtures, not only the temperature distributions but also the concentration distributions have a significant effect on the heat transfer. Therefore, heat and mass transfer should be considered simultaneously along with the phase-change process within the binary mixtures.

In this work, the absorption process within a heat exchanger (GAX absorber) with porous media was investigated. The absorption process was separated into three regions, a vapor region without porous media (region I), a vapor region within porous media (region II), and finally a liquid region within porous media (region III). For region I, heat transfer due to the temperature difference and the mass transfer due to the concentration difference were based on Colburn-Drew's classical formulation of the local transport equation in binary condensation. For region II, the convective heat and mass transfer within porous media was modeled based on constant wall temperature boundary condition. For region III, the convective heat transfer within porous media was modeled based on constant wall heat flux boundary condition.

The objectives of this article are to develop a countercurrent model for GAX absorber that includes the absorption process within the porous medium. The approximate effects of thermal conductivity and the porosity of the porous media on the absorption rate will also be investigated, and the Nusselt number within each region is obtained. These results can be applied for practical design of a GAX absorber.

DESCRIPTION OF SYSTEM

Kang and Christensen [11] developed a countercurrent model for GAX absorber. The GAX cycle was first proposed by Altenkirch [12]. McGahey [13], Phillips [14], and Erickson [15] described the GAX cycle in detail. The GAX absorber may consist of three heat exchangers as shown in Figure 1. The bottom heat exchanger is the hydronically cooled heat exchanger; the middle transfers heat from the liquid solution to the rich solution leaving the bottom of the absorber. The top heat exchanger (GAHX) recovers the absorber heat, transferring it to the generator, which operates in the high-temperature range of 360 to 450 K. A tube-in-tube-type heat exchanger is used in this work. The outer diameter of the inside tube and the inner diameter of the outside tube are 2.2 and 3.56 cm, respectively. Figure 2 shows the thermal conditions and the flow directions for the countercurrent GAX absorber. The weak liquid solution enters from the top, and the ammonia vapor enters at the bottom of the absorber. The temperature of the liquid solution drops as it flows downward, while the vapor temperature increases as it flows counter to the liquid, i.e., upward. The ammonia vapor is absorbed into the liquid solution due to the concentration difference. An aqueous solution of K_2CO_3 (35%) is used as a coolant in the hydronically cooled sections. Typical temperature and concentration dur-

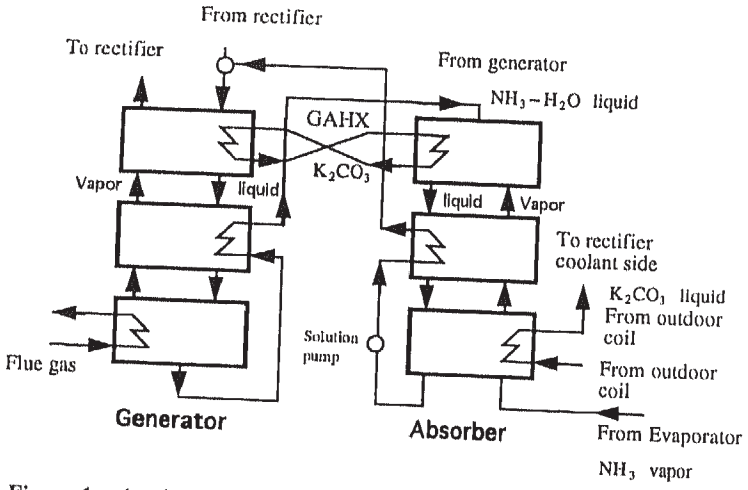

Figure 1 A schematic diagram of solution circuit for the GAX cycle.

ing countercurrent absorption are depicted in Figure 3.

As mentioned before, a porous medium is added along the wall to assist in eliminating the flooding phenomenon and decreasing heat transfer resistance. There are two regions within the porous media, namely, liquid and vapor regions. The other vapor region is within the core section of GAX absorber.

ANALYSIS

Heat Transfer Mechanisms during the Absorption Process

Figure 4 shows the heat and mass transfer components for an incremental section of the absorber assembly. For region I, heat transfer

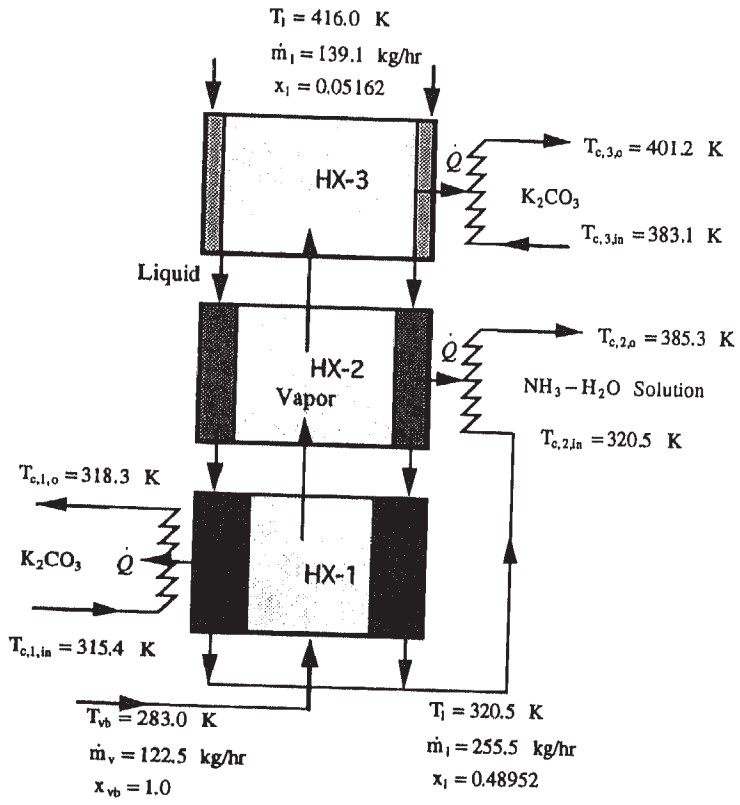

Figure 2 Thermal conditions and flow directions for the countercurrent GAX absorber.

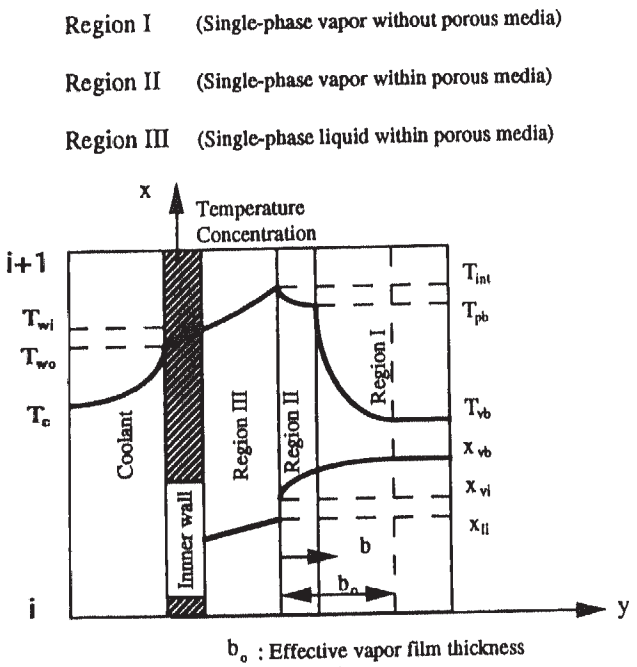

Figure 3 Typical temperature and concentration profiles during the countercurrent absorption process.

occurs from the interface to the bulk vapor region due to the absorption energy release at the interface. Within this region, forced-convection heat and mass transfer occur in single-phase vapor. Region II involves single-phase vapor transport through a porous medium. For this region, the interface temperature along the depicted incremental section is assumed to be constant. Strictly speaking, the interface temperature is a function of the length, L. However, since the interface temperature is the equilibrium temperature at a given pressure and concentration, the temperature can be assumed to be constant for a very small incremental length. Therefore, the interface temperature is approximated by a step function in this analysis.

Region III is modeled as external forced convection through a porous medium with constant wall heat flux. The constant wall heat flux results from the absorption heat release at the interface. The heat flux varies with length of the plane. However, as was the case for region II, the heat flux is approximately constant over a very small incremental length. Therefore, for region III, the heat flux at the interface is approximated by a step function.

Thermal Circuit for the Heat Transfer

Figure 5 shows the thermal circuit for the heat transfer during the absorption process. Heat transfer occurs in two directions. Heat transfer occurs from the interface to the coolant and also from the interface to the bulk vapor. In Figure 5, H_c is the heat transfer coefficient at the coolant side, and H_g, H_{pv}, and H_{pl} are heat transfer coefficients for regions I, II, and III, respectively.

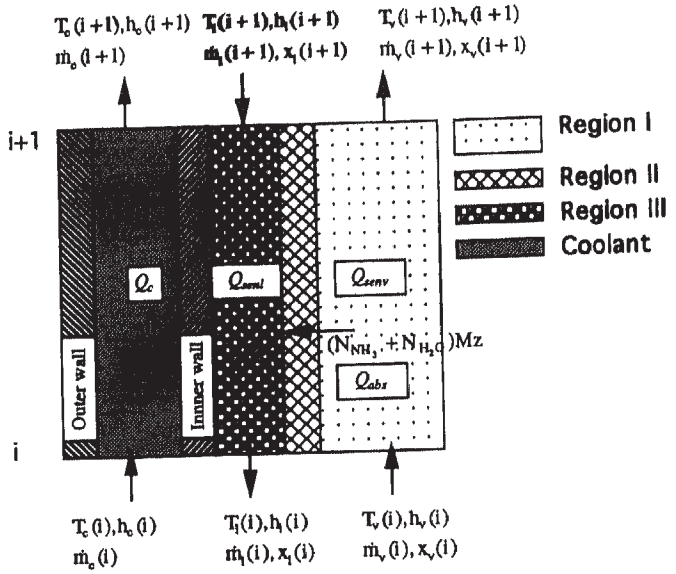

Figure 4 Heat and mass transfer components for an incremental section.

Governing Equations

Diffusion Equations for Region I

The net molar flux ammonia to the interface is the sum of flow transport and the molecular diffusion, which is given by

$$N_{NH_3} = (N_{NH_3} + N_{H_2O})x_v + \frac{\beta}{b_0} c \frac{dx_v}{d\eta} \tag{1}$$

where N is molar mass flux, x_v $(= c_{NH_3}/c)$ is the concentration, c is total molar density, η $(= b/b_0)$ is the nondimensional distance through the film, and b is a coordinate shown in Figure 3. In Eq. (1), diffusivity for polar gases, β, is calculated using the following equation given by Sherwood et al. [16]:

$$\beta = \frac{10^{-3} T^{1.75} \left[(M_{NH_3} + M_{H_2O})/(M_{NH_3} M_{H_2O}) \right]^{1/2}}{P \left[(\epsilon_{vNH_3})^{1/3} + (\epsilon_{vH_2O})^{1/3} \right]^2} \tag{2}$$

where β is in cm^2/s, T is in K, P is in atm, and ϵ_v is atomic diffusion volume in cm^3, $\epsilon_{vNH_3} = 14.9$ and $\epsilon_{vH_2O} = 12.7$. By introducing the molar composition of the absorbing vapor, z,

$$z = \frac{N_{NH_3}}{N_{NH_3} + N_{H_2O}} \tag{3}$$

and then combining Eqs. (1) and (3),

$$(N_{NH_3} + N_{H_2O})\, d\eta = \frac{\beta}{b_0} c \frac{dx_v}{z - x_v} \tag{4}$$

is obtained. Colburn and Drew [17] and Treybal [18] suggested that the $(\beta/b_0)c$ of Eq. (4), which is characteristic of molecular diffusion, can be replaced by F, a mass transfer coefficient. Integration of Eq. (4) gives

$$\int_0^1 (N_{NH_3} + N_{H_2O})\, d\eta = F \int_{x_{vi}}^{x_{vb}} \frac{dx_v}{(z - x_v)} \tag{5a}$$

or

$$N_{NH_3} + N_{H_2O} = F \ln\left(\frac{z - x_{vi}}{z - x_{vb}} \right) \tag{5b}$$

In Eq. (5), the mass transfer coefficient, F, was obtained using the Chilton-Colburn analogy [19] for turbulent flow as

$$F = 0.023 \left(\frac{DG_v}{\mu_v} \right)^{-0.2} \left(\frac{G_v}{M} \right) \left(\frac{\mu_v}{\rho_v \beta} \right)^{-2/3} \tag{6}$$

Overall Concentration Equation

The concentration balances of the ammonia vapor and liquid for the control volume (regions I, II, and III in Figure 4) are given by

$$\dot{m}_v(i) x_v(i) = \left[(N_{NH_3} + N_{H_2O}) M \right] \cdot z \cdot \Delta A + \dot{m}_v(i+1) \cdot x_v(i+1) \tag{7}$$

and

$$\dot{m}_l(i) \cdot x_l(i) = \left[(N_{NH_3} + N_{H_2O}) M \right] \cdot z \cdot \Delta A + \dot{m}_l(i+1) \cdot x_l(i+1) \tag{8}$$

respectively.

Overall Mass Balance Equations

The mass balance equations of vapor and liquid regions for the control volume are given by

$$\dot{m}_v(i) = \left[(N_{NH_3} + N_{H_2O}) M \right] \cdot \Delta A + \dot{m}_v(i+1) \tag{9}$$

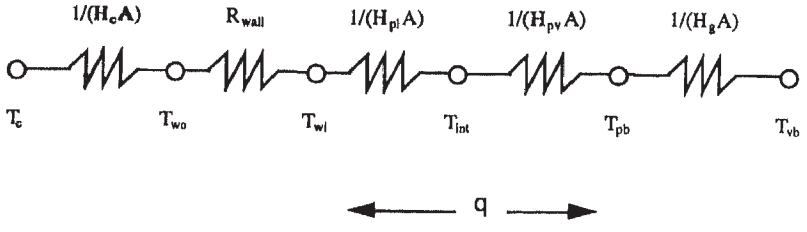

Figure 5 Thermal circuit for heat transfer during the absorption process.

and

$$\dot{m}_l(i) = \left[(N_{NH_3} + N_{H_2O})M\right] \cdot \Delta A + \dot{m}_l(i+1) \tag{10}$$

respectively.

Overall Energy Balance Equation

The overall heat transfer balance can be written by the following equation based on the control volume (regions I, II, and III) in Figure 4.

$$\begin{aligned} Q_c &= \left[\dot{m}_l(i+1)h_l(i+1) - \dot{m}_l(i)h_l(i)\right] \\ &\quad - \left[\dot{m}_v(i+1)h_v(i+1) - \dot{m}_v(i)h_v(i)\right] \\ &= Q_{abs} + Q_{sen,l} - Q_{sen,v} \end{aligned} \tag{11}$$

where

$$Q_{abs} = \Delta\dot{m}_{abs}\left[h_v(i) - h_l(i)\right] \tag{12}$$

$$Q_{sen,l} = \dot{m}_l(i+1)\left[h_l(i+1) - h_l(i)\right] \tag{13}$$

$$Q_{sen,v} = \dot{m}_v(i+1)\left[h_v(i+1) - h_v(i)\right] \tag{14}$$

and

$$\begin{aligned} \Delta\dot{m}_{abs} &= \dot{m}_v(i) - \dot{m}_v(i+1) \\ &= \dot{m}_l(i) - \dot{m}_l(i+1) \end{aligned} \tag{15}$$

where Q_c is the net heat transfer rate to the coolant, Q_{abs} is the heat transfer due to the absorption heat, $Q_{sen,l}$ is the sensible heat transfer rate defined in Eq. (13) for the liquid region, and $Q_{sen,v}$ is the sensible heat transfer rate defined in Eq. (14) for the bulk vapor region.

The total energy transferred to the interface from the bulk vapor per unit area is the sum of the absorption and sensible heat due to the absorbing vapor flow, which is given by

$$q_t = q_{abs} - q_{sen,v} \tag{16}$$

Since the sensible heat flux from the bulk vapor to the interface is the sum of the heat flux due to the vapor flow and conduction through the vapor film, $q_{sen,v}$ is given by the following equation:

$$\begin{aligned} q_{sen,v} &= H_g\left(-\frac{dT}{db}\right) \cdot b_0 + \left(N_{NH_3}M_{NH_3}C_{pNH_3}\right. \\ &\quad \left. + N_{H_2O}M_{H_2O}C_{pH_2O}\right)(T_{int} - T) \end{aligned} \tag{17}$$

By rearranging and integrating from 0 to b_0, and T_{int} to T_{vb},

$$q_{sen,v} = \frac{C_0(T_{int} - T_{vb})}{1 - e^{-C_0/H_g}} \tag{18}$$

where

$$C_0 = N_{NH_3}M_{NH_3}C_{pNH_3} + N_{H_2O}M_{H_2O}C_{pH_2O} \tag{19}$$

Now, the absorption heat flux, q_{abs}, is written by the following equation:

$$\begin{aligned} q_{abs} &= \left(N_{NH_3} + N_{H_2O}\right) \cdot M \cdot \lambda \\ &= F \cdot \ln\left(\frac{z - x_{vi}}{z - x_{vb}}\right) \cdot M \cdot \lambda \end{aligned} \tag{20}$$

where λ is the absorption heat during the absorption process, which is given by the following equation:

$$\lambda = h_v(T_{vb}) - h_l(T_{int}) \tag{21}$$

Therefore, the total energy transferred to the interface from the bulk vapor, q_t, is written by

$$q_t = F \cdot \ln\left(\frac{z - x_{vi}}{z - x_{vb}}\right) \cdot M \cdot \lambda - \frac{C_0(T_{int} - T_{vb})}{1 - e^{-C_0/H_g}} \tag{22}$$

The sum of q_t and $q_{sen,l}$ is the total energy picked up by the coolant per unit area, that is,

$$q_c = q_t + q_{sen,l} = U \cdot \text{LMTD} \tag{23}$$

where

$$U = \frac{1}{1/H_c + R_w + 1/H_{pl}} \tag{24}$$

and

$$\text{LMTD} = \frac{\left[T_{int}(i+1) - T_c(i+1)\right] - \left[T_{int}(i) - T_c(i)\right]}{\ln\left\{\left[T_{int}(i+1) - T_c(i+1)\right]/\left[T_{int}(i) - T_c(i)\right]\right\}} \tag{25}$$

Prediction of Nusselt Numbers in Each Region

For region I, the established heat transfer coefficient correlation for single-phase vapor can be

used for turbulent flow [20]. This is given by

$$H_g = 0.023\left(\frac{DG_v}{\mu_v}\right)^{-0.2} C_{pv}G_v\left(\frac{\mu_v C_{pv}}{k_v}\right)^{-2/3} \tag{26}$$

For region II, the governing equations can be written by

$$\frac{\partial u}{\partial x} + \frac{\partial v}{\partial y} = 0 \tag{27a}$$

$$u = -\frac{K}{\mu_v}\frac{\partial p}{\partial x} = U_v \qquad v = -\frac{K}{\mu_v}\frac{\partial p}{\partial y} = 0 \tag{27b}$$

$$U_v\frac{\partial T}{\partial x} = \alpha_v\frac{\partial^2 T}{\partial y^2} \tag{27c}$$

By introducing the following nondimensional parameters,

$$\zeta = \frac{y}{x}\left(\frac{U_v x}{\alpha_v}\right)^{1/2} \qquad \theta = \frac{T - T_{\text{int}}}{T_{vb} - T_{\text{int}}} \tag{28}$$

the energy equation and the boundary conditions reduce to

$$\theta'' + \frac{\zeta}{2}\theta' = 0 \tag{29a}$$

$$\theta(0) = 0 \qquad \theta(\infty) = 1 \tag{29b}$$

The above equations yield an error function solution given by

$$\theta = \text{erf}\left(\frac{\zeta}{2}\right) \tag{30}$$

$$\text{Nu}_x = 0.564\,\text{Pe}_x^{1/2} \tag{31}$$

The overall Nusselt number can then be expressed by

$$\overline{\text{Nu}}_L = 1.128\,\text{Pe}_L^{1/2} \tag{32}$$

Equation (32) can be used to calculate the heat transfer coefficient between the interface and the upper boundary of the porous media, that is, H_{pv}.

For region III, the governing equation and the boundary conditions are given by

$$u = -\frac{K}{\mu_l}\frac{\partial p}{\partial x} = U_l \qquad v = -\frac{K}{\mu_l}\frac{\partial p}{\partial y} = 0 \tag{33a}$$

$$U_l\frac{\partial T}{\partial x} = \alpha_l\frac{\partial^2 T}{\partial y^2} \tag{33b}$$

By introducing the following nondimensional parameters,

$$\xi = \frac{y}{x}\left(\frac{U_l x}{\alpha_l}\right) \qquad \theta = \frac{T - T_{\text{int}}}{q(U_{vb}x/\alpha_l)^{-1/2}\cdot(x/k_l)} \tag{34}$$

the governing equation and the boundary condi-

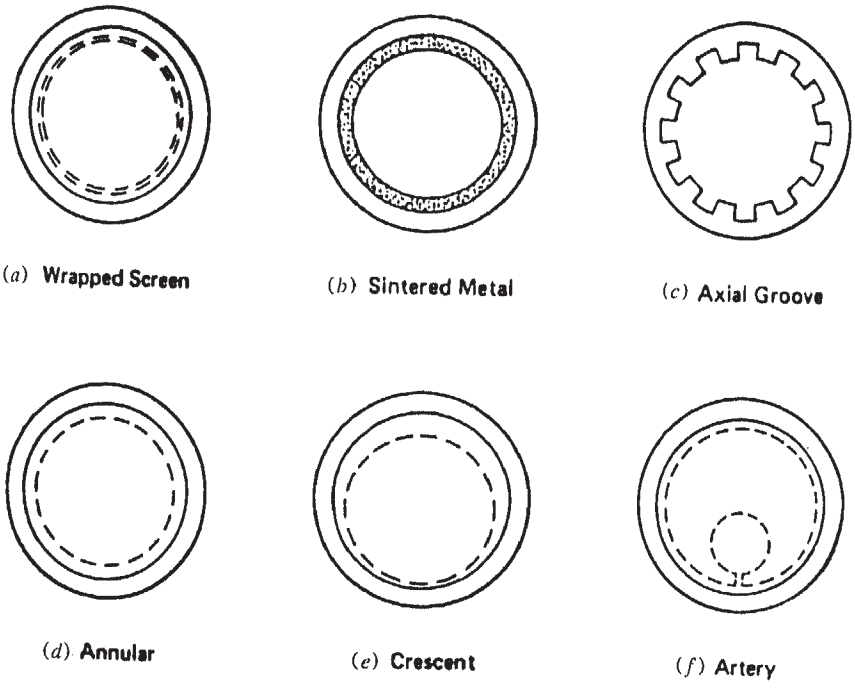

Figure 6 Cross section of homogeneous wick structure.

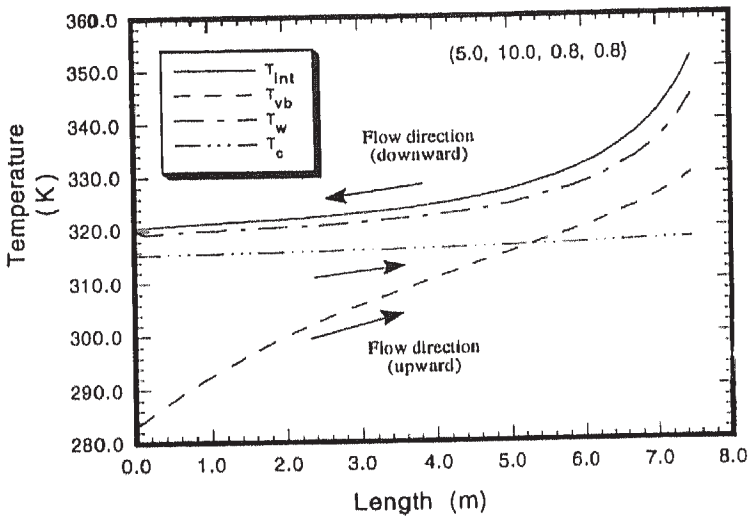

Figure 7 Temperature profiles of the absorber as a function of length.

tions reduce to

$$2\theta'' + \xi\theta' - \theta = 0 \tag{35a}$$

$$\theta'(0) = 1 \qquad \theta(\infty) = 0 \tag{35b}$$

Nield and Bejan [21] obtained the following equation for the local Nusselt number based on Eqs. (34) and (35):

$$\mathrm{Nu}_x = 0.886\,\mathrm{Pe}_x^{1/2} \tag{36}$$

The overall Nusselt number can be expressed by

$$\overline{\mathrm{Nu}}_L = 1.329\,\mathrm{Pe}_L^{1/2} \tag{37}$$

Equation (37) can be used to calculate the overall heat transfer coefficient between the interface and the coolant, that is, H_{pl}.

WICK STRUCTURES OF THE POROUS MEDIA

The purpose of a wick is to provide (1) the necessary flow passages, (2) surface pores at the liquid–vapor interface for the development of the required capillary pumping pressure, and (3) a heat flow path between the inner wall of the heat exchanger and the liquid–vapor interface. Chi [22] proposed that an effective wick structure requires small surface pores for large capillary pressure, large internal pores for minimal liquid flow resistance, and an uninterrupted highly conductive heat flow path across the wick thickness for a small temperature drop. Various types of wick structures have been developed based on satisfying these requirements.

Figure 6 shows several examples of homogeneous wick structure. The most common wick structure is the wrapped-screen wick shown in Figure 6. In this study, the wrapped-screen wick structure was adopted for regions II and III. For the wrapped-screen wick structure, the effective thermal conductivity is given by the following set of equations:

$$k_{el} = \frac{k_l\left[(k_l + k_p) - (1 - \mathrm{el})(k_l - k_p)\right]}{(k_l + k_p) + (1 - \mathrm{el})(k_l - k_p)} \tag{38}$$

$$k_{ev} = \frac{k_v\left[(k_v + k_p) - (1 - \mathrm{ev})(k_v - k_p)\right]}{(k_v + k_p) + (1 - \mathrm{ev})(k_v - k_p)} \tag{39}$$

where el and ev are the porosities of the porous media in liquid and vapor regions, respectively. Tien and Vafai [23] proposed another precise relationship for the effective thermal conductivity within the porous media based on the use of two variational principles and a perturbation expansion. The results of such an analysis is given in terms of the thermal conductivity ratio of the two phases, the porosity, and a geometric factor that depends on the geometric unit structure of the porous matrix.

RESULTS AND DISCUSSION

The bottom section of the GAX absorber (HX-1 in Figure 2) was considered in this study, but in

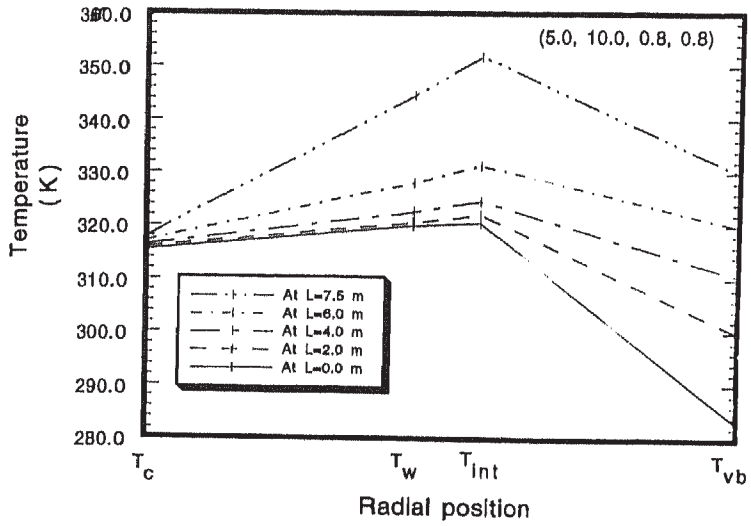

Figure 8 Temperature profiles of the absorber as a function of radial positions.

principle this analysis can be applied to the other sections as well. Figure 7 shows the temperature profiles along the tube length. The quantity in parentheses in each figure represents (rkl, rkv, el, ev), where rkl ($= k_p/k_l$) is the ratio of thermal conductivity of porous medium to that of the liquid solution, rkv ($= k_p/k_v$) is the ratio of thermal conductivity of the porous medium to that of the vapor solution, and el and ev are the porosities of the porous media in the liquid and vapor regions, respectively. Due to the counter-current flow between the liquid and vapor flow in the GAX absorber, the temperature difference between the interface and bulk vapor decreases along the length of the tube. Even though the temperature difference between the interface and bulk vapor decreases with an increase in the length of the tube, the concentration difference increases because the dependence of the liquid concentration on the interface temperature is more prominent than that of the bulk vapor concentration on the bulk vapor temperature. As a result, the interface temperature profile had the same trend as the absorption rate, and the absorption rate increased with an increase in the tube length (see Figures 11–14). Figure 8 shows the temperature profiles in the radial direction. The interface temperature is the highest due to the heat absorption near the interface. While the vapor temperature was lower than the coolant temperature at the

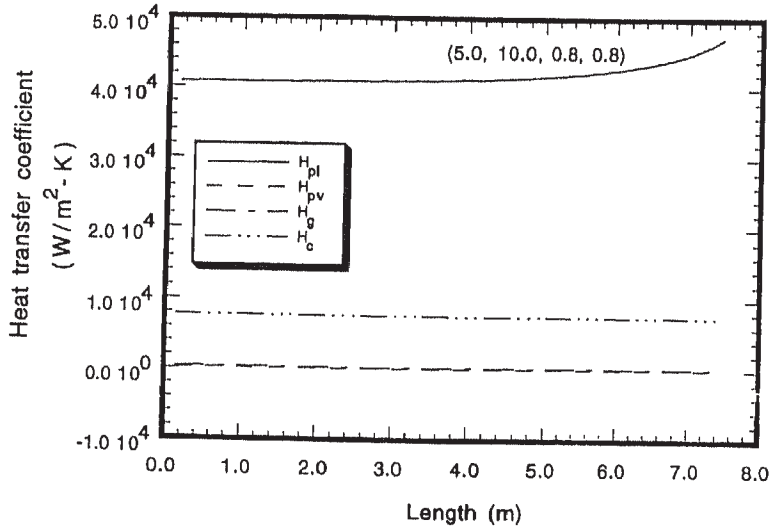

Figure 9 Heat transfer coefficients of the absorber at each region.

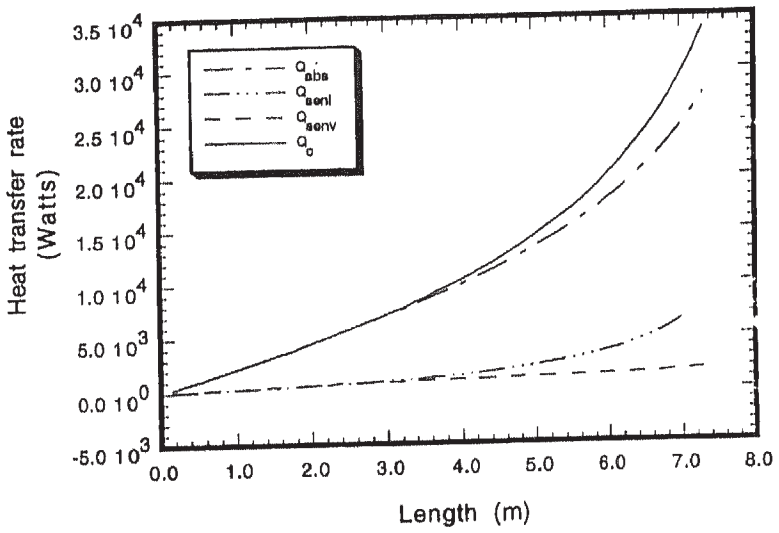

Figure 10 The amount of each heat transfer load.

entrance section of the vapor, the vapor temperature became higher than the coolant temperature after $L = 5.3$ m due to the sensible heat from the interface to the bulk vapor.

Figure 9 shows the heat transfer coefficients for each region. The heat transfer coefficient in region III (H_{pl}) was much larger than the others. The heat transfer occurs in two directions as shown in Figure 5. The dominant heat transfer coefficient would be the coolant side (H_c) rather than the H_{pl}, because the net heat load transferred to the coolant is leftward in Figure 5. Even though the heat transfer coefficient for coolant side, H_c, had the dominant effect on the overall heat transfer coefficient, U, the other coefficients also had significant effect on the absorption rate, which in turn determines the tube length. This is because the heat transfer coefficients in region II (H_{pv}) and in region I (H_g) have significant effects on the bulk vapor temperature, and the temperature difference between the interface and the bulk vapor region affects the absorption rate directly. Figure 10 shows variations of the Q_{abs}, Q_{senl}, Q_{senv}, and Q_c along the length of the tube. The sensible heat for the vapor region was small compared with the other heat loads due to the low heat transfer coefficient in the vapor region.

Figure 11 shows the effect of the ratio of the thermal conductivity of the porous medium to that of the liquid solution (rkl) on the absorption rate. As expected, rkl has a significant effect on the absorption rate and the required length of the

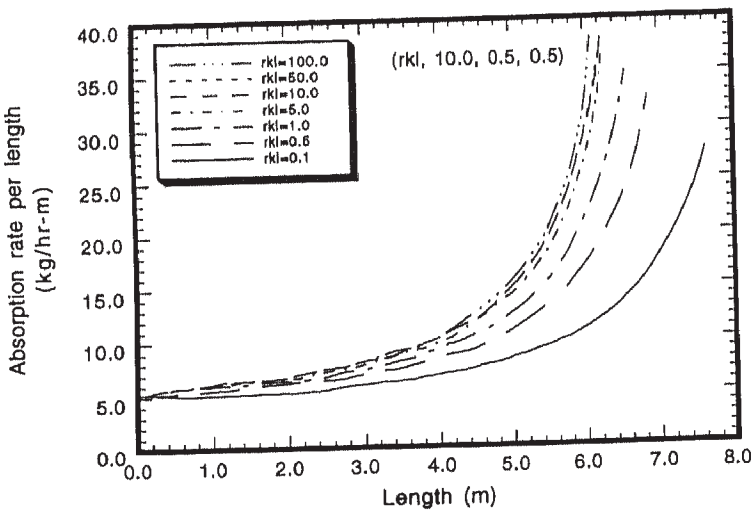

Figure 11 The effect of thermal conductivities of the porous matrix in the liquid region on the absorption rate.

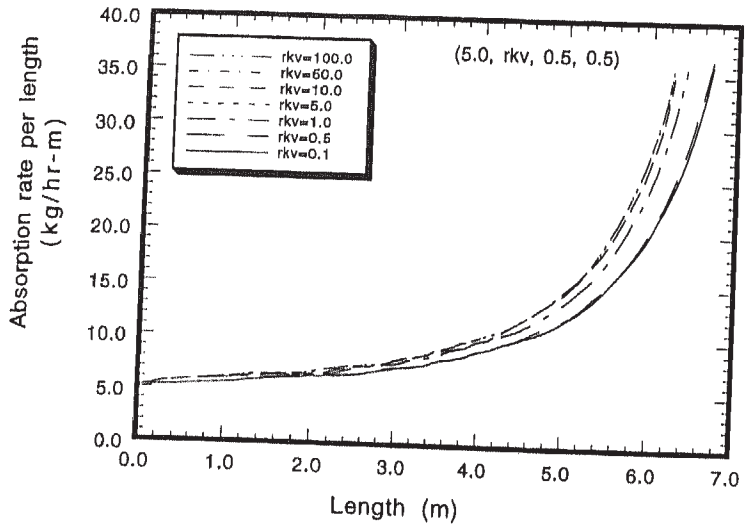

Figure 12 The effect of thermal conductivities of the porous matrix in the vapor region on the absorption rate.

tube. As shown in Figure 11, the absorption rate increases with an increase in the ratio of the thermal conductivity. However, the rate of increase of the absorption rate with the ratio of thermal conductivity tapers off after rkl = 5.0. Therefore, rkl = 5.0 is the optimum value in designing the GAX absorber. Figure 12 shows the effect of ratio of the thermal conductivity of the porous medium to that of the vapor solution (rkv) on the absorption rate. It should be noted, as seen in Figures 11 and 12, that the heat exchanger size has a minimal effect on the vapor heat transfer coefficient while it has a significant effect on the liquid heat transfer coefficient. It can be said that rkv = 5.0 is also the optimum value in designing the GAX absorber, as seen in Figure 12.

Figures 13 and 14 show the effects of the porosities of the porous media on the absorption rate and the required length of the tube. The absorption rate decreases with an increase in the porosity of the porous medium. This is due to significantly larger thermal conductivity of the solid compared to that of the liquid and the much higher velocity of the liquid solution with the smaller porosity. From Figures 13 and 14, it was found that porosity of 0.2 is the minimum value to get the higher absorption rate leading to a smaller size of the heat exchanger. The pressure drop through the heat exchanger would be very high when the porosity is small. Therefore, it can be said that the optimum value of the porosity of the porous medium should be larger than 0.2.

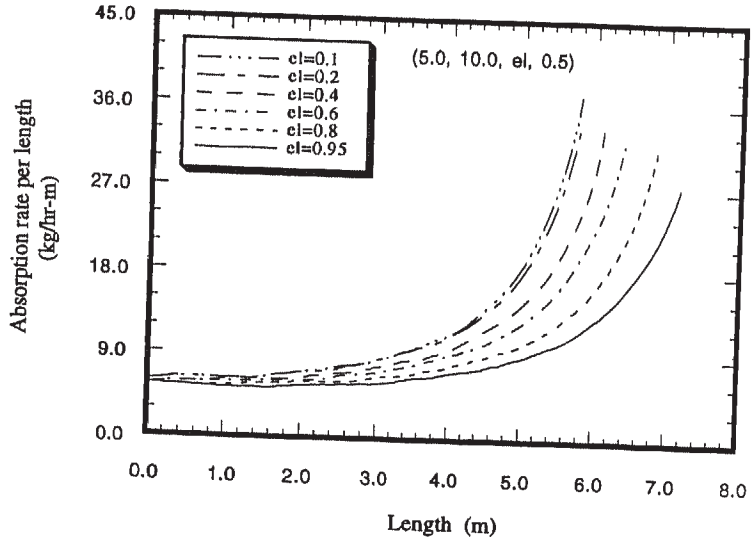

Figure 13 The effect of porosities of the porous matrix in the liquid region on the absorption rate.

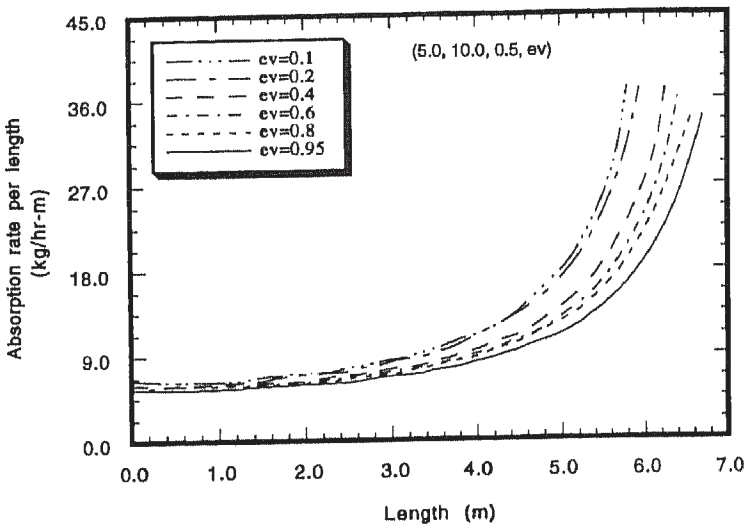

Figure 14 The effect of porosities of the porous matrix in the vapor region on the absorption rate.

CONCLUSIONS

1. A countercurrent model for GAX absorber that includes the absorption process within porous media is proposed. The heat and mass transfer was considered in three regions. These were a single-phase vapor region without porous media, a single-phase vapor region within porous media, and a single-phase liquid region within porous media. This analysis can be applied for practical design of a GAX absorber.
2. It was proposed that the flooding phenomena at the liquid–vapor interface can be removed using a porous medium. It was found that when the porous medium is used in designing the GAX absorber, the heat transfer coefficients H_{pv} and H_g had a significant effect on the absorption rate.
3. The effects of the ratio of conductivities of the porous matrix to those of the liquid and vapor on the absorption rate and the required tube length were investigated. As expected, it was found that the absorption rate increases and the required tube length is reduced as the ratio of conductivities increases. It was also found that the optimum value of the ratio of the thermal conductivities is 5.0.
4. The effect of the porosity on the absorption rate and required tube length was also investigated. The absorption rate increases and the required tube length is reduced with a decrease in porosity. It was found that the optimum value of the porosity of the porous medium should be larger than 0.2. Therefore, a porous medium with higher thermal conductivity and a smaller porosity (but larger than 0.2) is required to obtain a higher absorption rate, leading to a smaller size of the heat exchanger.

NOMENCLATURE

A	heat transfer area, m^2
b	coordinate shown in Figure 3
b_0	effective vapor film thickness, m
c	total molar density, kg mol/m^3
c_{NH_3}	molar density of NH_3, kg mol/m^3
C_p	specific heat, J/kg K
D	diameter of inside tube, m
el, ev	porosities of porous media at liquid and vapor regions
F	mass transfer coefficient, kg mol/m^2 s
G	mass velocity, kg/m^2 s
H_c, H_g, H_{pl}, H_{pv}	heat transfer coefficients at coolant, bulk vapor, liquid within porous media, and vapor within porous media regions, respectively, W/m^2 K
k	thermal conductivity, W/m K
k_{el}, k_{ev}	effective thermal conductivities at liquid and vapor regions within porous media, W/m K
K	permeability of a porous medium, m^2
L	length, m

LMTD	log mean temperature difference, K
m	mass flow rate, kg/hr
M	mean molecular weight, kg/kg mol
M_{H_2O}, M_{NH_3}	molecular weight of water and ammonia, respectively, kg/kg mol
N	mass flux, kg mol/m^2 s
Nu	Nusselt number
p	pressure, N/m^2
Pe	Peclet number
q	energy transferred rate per unit area, W/m^2
Q	heat transfer rate, W
R_w	thermal resistance of the tube wall, W^{-1} K
T	temperature, K
u, v	velocities in x and y directions, respectively, m/s
U	overall heat transfer coefficient, W/m^2 K
U_l, U_v	mean velocities of liquid and vapor respectively, m/s
x, y	coordinates in Figure 3
x_l, x_v	molar concentration for NH_3 for liquid and vapor, respectively
z	composition of ammonia on a molar basis
α	thermal diffusivity, m^2/s
β	diffusion coefficient, m^2/s
ϵ	atomic diffusion volume, m^3
ζ	nondimensional parameter in Eq. (28)
η	distance ratio, b/b_0
θ	nondimensional temperature
λ	absorption heat defined in Eq. (19), J/kg
μ	dynamic viscosity, kg/m s
ξ	nondimensional parameter in Eq. (34)
ρ	density, kg/m^3

Subscripts

abs	absorption
c	coolant
int	interface
l	liquid
p	porous matrix
pb	upper boundary of porous medium
pl, pv	liquid and vapor within porous medium, respectively
sen$l$	sensible heat in the liquid region
sen$v$	sensible heat in the vapor region
t	total
v	vapor
vb	bulk vapor
w	wall
wi, wo	inner and outer wall surfaces

REFERENCES

[1] Hewitt, G. F., *Handbook of Heat Exchanger Design*, Hemisphere, New York, Chap. 2.6, 1990.

[2] Tien, C. L., and Vafai, K., Convective and Radiative Heat Transfer in Porous Media, *Adv. Appl. Mech.*, vol 27, pp. 225–281, 1990.

[3] Vafai, K., and Whitaker, S., Simultaneous Heat and Mass Transfer Accompanied by Phase Change in Porous Insulation, *J. Heat Transfer*, vol. 108, pp. 132–140, 1986.

[4] Vafai, K., and Sarjar, S., Condensation Effects in a Fibrous Insulation Slab, *J. Heat Transfer*, vol. 108, pp. 667–675, 1986

[5] Vafai, K., and Sozen, M., Analysis of Energy and Momentum Transport for Fluid Flow through a Porous Bed, *J. Heat Transfer*, vol. 112, pp. 690–699, 1990.

[6] Vafai, K., and Sozen, M., An Investigation of a Latent Heat Storage Porous Bed and Condensing Flow through It, *J. Heat Transfer*, vol. 112, pp. 1014–1022, 1990.

[7] Sozen, M., and Vafai, K., Analysis of the Non-thermal Equilibrium Condensing Flow of a Gas through a Packed Bed, *Int. J. Heat Mass Transfer*, vol. 33, no. 6, pp. 1247–1261, 1990.

[8] Vafai, K., and Tien, H. C., A Numerical Investigation of Phase Change Effects in Porous Materials, *Int. J. Heat Mass Transfer*, vol. 32, no. 7, pp. 1261–1277, 1989.

[9] Kaviany, M., *Principles of Heat Transfer in Porous Media*, Springer-Verlag, chap. 12, 1991.

[10] Cheng, P., Film Condensation along an Inclined Surface in a Porous Medium, *Int. J. Heat Mass Transfer*, vol. 24, no. 6, pp. 983–990, 1981.

[11] Kang, Y. T., and Christensen, R. N., Development of a Counter-Current Model for a Vertical Fluted Tube GAX Absorber, *ASME, Proceedings of the International Absorption Heat Pump Conference*, AES vol. 31, pp. 7–16, 1994.

[12] Altenkirch, E., Reversible Absorptionsmachinen, *Z. ges. Kalte-Industrie*, vol. XX, 1913.

[13] McGahey, K., The Modeling and Optimization of a Generator-Absorber Heat Exchanger, Absorption Heat Pump Using a Modular Steady State Simulation, M.S. thesis, The Ohio State University, Columbus, OH, 1993.

[14] Phillips, B. A., Development of an Advanced-Cycle Absorption Heat Pump for Residential Applications, *Proc. 2nd DOE / ORNR Heat Pump Conf.*, CONF-8804100, 1988.

[15] Erickson, D. C., Branched GAX Absorption Vapor Compression, U.S. Patent 5024063, 1991.

[16] Sherwood, T. K., Pigford, R. L., and Wilke, C. R., *Mass Transfer*, McGraw-Hill, New York, chap. 2, 1975.
[17] Colburn, A. P., and Drew, T. B., The Condensation of Mixed Vapor, *Trans. AIChE*, vol. 33, pp. 197–215, 1937.
[18] Treybal, R. E., *Mass-Transfer Operations*, 2d ed., McGaw-Hill, New York, chap. 3, 1968.
[19] Chilton, T. H., and Colburn, A. P., Mass Transfer (Absorption) Coefficients, Prediction from Data on Heat Transfer and Fluid Friction, *Ind. Eng. Chem.*, vol. 26, pp. 1183–1187, 1934.
[20] Colburn, A. P., A Method of Correlating Forced Convection Heat Transfer Data and a Comparison with Fluid Friction, *Trans. AIChE*, vol. 29, pp. 174–209, 1933.
[21] Nield, D. A., and Bejan, A., *Convection in Porous Media*, Springer-Verlag, chap. 4, 1992.
[22] Chi, S. W., *Heat Pipe Theory and Practice*, Hemisphere, chap. 1, 1976.
[23] Tien, C. L., and Vafai, K., Statistical Bounds for the Effective Thermal Conductivity of Microsphere and Fibrous Insulation, *AIAA Prog. Ser.*, vol. 65, pp. 135–148, 1978.

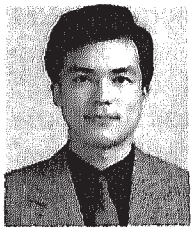

Yong Tae Kang is a postdoctoral researcher at the department of mechanical engineering, Ohio State University. He received BS (1987) and MS (1989) degrees from Seoul National University, Seoul, Korea, and a PhD from Ohio State University in 1994. He is an expert in absorption technology. He conducts research in combined heat and mass transfer analysis, heat pump components modeling, enhanced heat transfer, heat transfer in porous media, heat exchanger design, two-phase flow, and experimental and theoretical work on boiling and condensation.

Richard N. Christensen is a professor of mechanical engineering at the Ohio State University. He received a BS (1968) in physics from Brigham Young University, an MS (1972) in mechanical engineering and a PhD (1974) in nuclear engineering from Stanford University. He has published extensively in the areas of enhanced heat transfer, heat exchanger designs, absorption heat pump systems, boiling and condensation, thermal hydraulics, passive features of nuclear reactors, and condensation in the presence of noncondensable gas.

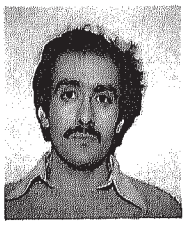

Kambiz Vafai started his bachelor's work in 1972 and acquired his BS in mechanical engineering from the University of Minnesota in 1975. He received his MS (1977) and PhD (1980) in mechanical engineering from the University of California at Berkeley. After spending a year as a postdoctoral fellow at Harvard University, he joined the Ohio State University's department of mechanical engineering in 1981. He was promoted to the rank of full professor in 1991 and became a Fellow of the American Society of Mechanical Engineers in 1992. Dr. Vafai has been an invited visiting professor at the Technical University of Munich in Germany and at the University of Bordeaux in France. Dr. Vafai is the associate editor of the *ASME Journal of Heat Transfer*, and he is also on the editorial board of the *International Journal of Heat and Fluid Flow*. Dr. Vafai has published extensively in the areas of transport through porous media and multiphase transport, natural convection in complex configurations, analysis of porous insulations, high energy storage and recovery, and free surface flows.